JOURNAL OF VIROLOGY, Feb. 2001, p. 1236–1251 Vol. 75, No. 3
0022-538X/01/$04.00+0 DOI: 10.1128/JVI.75.3.1236–1251.2001

Characterization of Herpes Simplex Virus-Containing Organelles by Subcellular Fractionation: Role for Organelle Acidification in Assembly of Infectious Particles

CAROL A. HARLEY, ANINDYA DASGUPTA, AND DUNCAN W. WILSON*

Department of Developmental and Molecular Biology, Albert Einstein College of Medicine, Bronx, New York 10461

Received 26 September 2000/Accepted 7 November 2000

The cytoplasmic compartments occupied by exocytosing herpes simplex virus (HSV) are poorly defined. It is unclear which organelles contain the majority of trafficking virions and which are occupied by virions on a productive rather than defective assembly pathway. These problems are compounded by the fact that HSV-infected cells produce virus continuously over many hours. All stages in viral assembly and export therefore coexist, making it impossible to determine the sequence of events and their kinetics. To address these problems, we have established assays to monitor the presence of capsids and enveloped virions in cell extracts and prepared HSV-containing organelles from normally infected cells and from cells undergoing a single synchronized wave of viral egress. We find that, in both cases, HSV particles exit the nucleus and accumulate in organelles which cofractionate with the *trans*-Golgi network (TGN) and endosomes. In addition to carrying enveloped infectious virions in their lumen, HSV-bearing organelles also displayed nonenveloped capsids attached to their cytoplasmic surface. Neutralization of organellar pH by chloroquine or bafilomycin A resulted in the accumulation of noninfectious enveloped particles. We conclude that the organelles of the TGN/endocytic network play a key role in the assembly and trafficking of infectious HSV.

The mechanisms of envelopment and intracellular trafficking of herpes simplex virus (HSV) are poorly understood. A number of ultrastructural studies have shown that viral nucleocapsids containing packaged DNA are assembled in the infected cell nucleus and then bud through the inner nuclear membrane into the perinuclear space, acquiring an envelope (62, 63, 66). However, the interpretation of images representing subsequent stages in virus egress has been controversial. Electron microscopy reveals that the infected cell cytoplasm contains capsids partially wrapped by adjacent membranes, enveloped virions completely enclosed within membranous vesicles, and "naked" capsids entirely lacking envelopes (4, 14, 38, 41, 72).

Two principal HSV egress models have been proposed to account for these various cytoplasmic structures (27, 80). In one model, it has been suggested that perinuclear enveloped virions enter transport vesicles budding from the outer nuclear membrane or endoplasmic reticulum (ER) and then traffic as normal secretory pathway cargo through the Golgi apparatus and are eventually secreted from the cell (25, 38, 66, 72). In this model, naked cytoplasmic capsids arise due to nonproductive, erroneous deenvelopment, wherein the envelope of trafficking virions becomes fused with the surrounding lipid bilayer of the transport vesicle. Increased accumulation of naked capsids in the cytoplasm of cells infected by an HSV strain mutant in glycoprotein gD supports the view that premature fusion can generate nonenveloped capsids (14); however, it is not clear if such a phenomenon is the source of naked capsids during a wild-type viral infection.

* Corresponding author. Mailing address: Department of Developmental and Molecular Biology, Albert Einstein College of Medicine, 1300 Morris Park Avenue, Bronx, NY 10461. Phone: (718) 430 2305. Fax: (718) 430 8567. E-mail: wilson@aecom.yu.edu

In an alternative model (65), perinuclear virions undergo a programmed deenvelopment in which they fuse their envelopes with the outer nuclear membrane, releasing naked capsids into the cytoplasm. These capsids lie on a productive route of assembly and subsequently reenvelope by budding into the lumen of some organelle of the secretory or endocytic pathways (41). Consistent with this reenvelopment model are the recent observations that retention of either of the viral glycoproteins gH and gD in the ER prevents their incorporation into the envelopes of secreted virions (11, 79). Similarly, examination of the phospholipid composition of extracellular HSV particles revealed that the viral membrane is enriched in lipids which are most abundant in organelles other than the ER (76), and studies in explanted neurons have shown that the anterograde transport of HSV virions along axons appears to involve distinct pathways for nucleocapsid/tegument and glycoproteins (35, 36, 49, 55). Similar reenvelopment egress pathways have been proposed for other herpesviruses, based primarily on electron microscopic observations (15, 29, 30, 34, 39, 51, 71, 78, 84). Evidence for and against each of these models of egress has recently been comprehensively reviewed (27).

Whichever egress model is correct, the identity of those cytoplasmic organelles in which enveloped virions accumulate is unclear. Similarly, the kinetics with which capsids pass through the egress pathway and the relative abundance of naked and enveloped capsids in various cytoplasmic compartments are questions which have been difficult to address. One reason for this is that infected cells replicate HSV continuously for 18 to 24 h. They therefore contain viruses at every stage of assembly, making it impossible to determine the order of events during viral biogenesis. Furthermore, electron microscopic techniques cannot reveal whether a particular compartment contains infectious or defective particles.

We have described a model system to facilitate the study of

late events in HSV assembly. The HSV-1 strain *ts*Prot.A carries a reversible temperature-sensitive lesion in UL26, which encodes the maturational protease Pra (28, 48, 57, 58). At the nonpermissive temperature of 39°C, *ts*Prot.A-infected cells accumulate immature nuclear procapsids (54, 59). Following downshift to the permissive temperature of 31°C, these procapsids recruit the capsid subunit VP26 (21, 54), package DNA (22, 24, 57), and give rise to exocytosing infectious particles in a synchronous wave (23). In the present study, we make use of this synchronized assembly system, in combination with biochemical assays for packaged capsids and enveloped viral particles, to examine virus-containing organelles by differential ultracentrifugation. This has enabled us to characterize which cytoplasmic organelles are associated with infectious and noninfectious virions, to determine the relative abundance of capsids and enveloped virions in various compartments, and to monitor the kinetics with which exiting virus traverses the cytoplasm. Our data show that enveloped infectious virions accumulate in organelles with biochemical properties similar to those of the *trans*-Golgi network (TGN) and endosomes and that nonenveloped capsids are also tethered to the cytoplasmic face of these organelles. No HSV appeared to accumulate in earlier compartments of the Golgi apparatus or in lysosomes. Chloroquine or bafilomycin A1, which neutralize the acidic pH of the endosomal/recycling network, dramatically decreased the yield of infectious virions, even though the number of enveloped particles remained similar to untreated controls. We conclude that, under our conditions, TGN and/or endosomes are key organelles in HSV exocytosis and that an acidic pH is critical for cytoplasmic viral particles to acquire infectivity.

MATERIALS AND METHODS

Cells, media, and viruses. Human hepatoma (HuH7) cells were maintained in RPMI supplemented with 1% penicillin-streptomycin (PS) (Gibco Laboratories) and 10% fetal calf serum (FCS). Vero cells were grown in Dulbecco's modified Eagle's medium (DMEM)–1% PS supplemented with 10% newborn calf serum (NCS). The HSV-1 strains *ts*Prot.A and SC16 were prepared as previously described (23). Plaque assays were done by titration on preformed Vero cell monolayers. Chloroquine and brefeldin A (BFA) were obtained from Sigma, and bafilomycin A_1 was from Kamiya Biomedical, Seattle, Wash.

Western blotting and antibodies. Extracts were boiled in Laemmli buffer and then subjected to denaturing sodium dodecyl sulfate-polyacrylamide gel electrophoresis using 8 or 12% resolving gels. Proteins were transferred to a nitrocellulose membrane at 80 mA for 2 h with a Hoeffer semidry blotter, and then the membrane was blocked for 1 h at room temperature in Tris-buffered saline (150 mM NaCl, 10 mM Tris-HCl [pH 7.6]) supplemented with 0.5% Tween 20 and 5% nonfat dried milk. Membranes were then incubated overnight at 4°C with the appropriate antibody. Antibodies were obtained from the following sources: anti-βCOP monoclonal clone maD was from Sigma; affinity-purified anti-TGN46 antiserum was from Serotec; anti-γ-adaptin, anti-EEA1, and anti-rab5 (clone C1) monoclonals were from Transduction Laboratories; polyclonal anticalnexin was from Stressgen Biotech. Corp.; and anti-PCNA monoclonal clone PC10 was from Santa Cruz Biotechnology. For anti-LAMP1 monoclonal clone H4A3, anti-rab7, and anti-p115, see the Acknowledgments. Secondary antibody detection was done by Pierce Supersignal chemiluminescence.

Cell labeling and total-extract and PNS preparation. HuH7 cells at 70 to 80% confluence were incubated for 2 h at 37°C in RPMI medium containing 1% dialyzed FCS. They were then infected at a multiplicity of infection (MOI) of 10 with HSV strain *ts*Prot.A for 1 h at 37°C, and unpenetrated virus was inactivated by a wash with glycine-buffered saline (GBS; 136 mM NaCl, 5 mM KCl, 100 mM glycine [pH 2.8]), then overlaid with warmed RPMI–1% dialyzed FCS containing [^{3}H]thymidine at a final concentration of 25 μCi/ml, and incubated for a further 7 h at 39°C (nonpermissive temperature) before downshift to 31°C (permissive temperature). At 30 min prior to downshift, cycloheximide (20 μg/ml) was added to ensure a single pulse of viral assembly. To prepare total extracts, cells were rinsed twice in TBS_B (130 mM NaCl, 20 mM KCl, 25 mM Tris-HCl [pH 7.6]) and then frozen, thawed, collected by scraping, and sonicated. Alternatively, cells were rinsed twice in homogenization buffer (HB_A, 250 mM sucrose, 2 mM $MgCl_2$, 10 mM Tris-HCl [pH 7.6]) collected by scraping, homogenized by eight passages through a $25^{5/8}$-gauge needle, and then spun at 2,000 × *g* for 10 min at 4°C to remove unbroken cells and nuclei and yield a postnuclear supernatant (PNS).

Measurement of DNA packaging and capsid envelopment. The trichloroacetic acid (TCA) precipitation assay used to measure DNA packaging was modified from our earlier published study (24) as follows. Cell extracts or gradient fractions were incubated in the presence of 2 mM $MgCl_2$ and 280 U of DNase I (Sigma; type II) per ml for 90 min at 37°C. EDTA and SDS were then added to a final concentration of 10 mM and 0.3%, respectively, and incubation was continued for a further 15 min at 37°C before spotting onto individual GF/C Whatman filters. Each filter was subjected to one 4°C wash and two consecutive 65°C washes in TP buffer (5% TCA, 20 mM sodium pyrophosphate) before being rinsed in 70% ethanol at room temperature and dried. Levels of TCA-precipitable radioactivity were determined by liquid scintillation counting. To measure only that DNA present in enveloped capsids, samples were first incubated with 0.2 mg of proteinase K per ml for 90 min at 37°C to destroy nonenveloped capsids. The reaction was quenched by addition of 2 mM phenylmethylsulfonyl fluoride and then subjected to DNase I treatment and TCA precipitation as above.

Percoll density gradient centrifugation. Generally, four to five 15-cm dishes of HuH7 cells at 70 to 80% confluency were used for each gradient. Cells were washed twice with HB_A, and a PNS was prepared as described above. The PNS was mixed with stock Percoll solution to prepare 11 ml of a solution of 1.065 g of Percoll per ml in 250 mM sucrose, as per the manufacturer's instructions (Pharmacia Biotech). A self-forming gradient was produced by centrifugation for 45 min at 20,000 rpm (36,000 × *g*) in a Ti50 fixed-angle rotor at 4°C, and 22 0.5-ml fractions were collected from the top of the gradient.

Sucrose float-up gradients. Cells were washed twice with HB_A, and 1 ml of PNS was prepared as described above, of which 0.9 ml was adjusted to 1.4 M sucrose and loaded onto a step gradient as follows: 1 ml of 2 M sucrose overlaid with 2 ml of 1.4 M adjusted PNS, 7.5 ml of 1.2 M sucrose, and 1.5 ml of 0.8 M sucrose; all solutions contained 10 mM Tris-HCl (pH 7.6) and 2 mM $MgCl_2$. The gradient was centrifuged for 4 h at 39,000 rpm (261,000 × *g*) in an SW41 rotor at 4°C, and 12 1-ml fractions were collected from the top of the gradient.

HRP uptake to label endocytic compartments. After 16 h of HSV infection, HuH7 cells were washed three times with warmed serum-free RPMI. Serum-free RPMI containing 1.4 mg of horseradish peroxidase (HRP; obtained from Sigma) per ml was then added to each dish, and the cells were incubated at 37°C for 12 min. The cells were subsequently transferred to ice and washed five times (2 min per wash) with cold phosphate-buffered saline (PBS)–1 mM $MgCl_2$–1 mM $CaCl_2$–0.1% bovine serum albumin (BSA) and then washed twice with HB_A. The cells were scraped from the dish into HB_A, and a PNS was prepared and fractionated as described above. Gradient fractions were blotted onto a nitrocellulose membrane using a Hoeffer vacuum blotting apparatus, and bound HRP was detected directly by incubation of the membrane with Supersignal Chemiluminescence (Pierce).

Measurement of Golgi glycosyltransferase activities in gradient fractions. Galactosyltransferase activity was determined as described by Chaney and colleagues (16). Sialyltransferase activity was measured by incubating each gradient fraction with asialofetuin (20 mg/ml; Sigma) in 1.25% Triton X-100–50 mM MOPS (morpholinopropanesulfonic acid, pH 6.5)–5 mM $MnCl_2$–1 mM CMP-[^{3}H]sialic acid (New England Nuclear; adjusted to a final specific activity of 2,000 cpm/nmol using unlabeled CMP-sialic acid from Sigma) for 1 h at 37°C. The reaction was stopped by addition of 1 ml of ice-cold water, and then samples were TCA precipitated onto GF/C filters, and precipitable cpm were determined by liquid scintillation counting.

Transmission electron microscopy. Fractions from sucrose float-up gradients were pelleted in an Airfuge at ~26 lb/in^2 for 20 min at 4°C. The pellet was fixed in 2.5% glutaraldehyde in SC (100 mM sodium cacodylate [pH 7.43]) at room temperature for 45 min, rinsed in SC, postfixed in 1% osmium tetroxide in SC followed by 1% uranyl acetate, dehydrated through a graded series of ethanols, and embedded in LX112 resin (LADD Research Industries, Burlington, Vt.). Ultrathin sections were cut on a Reichert Ultracut E, stained with uranyl acetate followed by lead citrate, and viewed on a Joel 1200EX transmission electron microscope at 80 kV.

RESULTS

Development of rapid biochemical assays to detect packaged and enveloped capsids. We first wished to develop a rapid and quantitative means of assaying for the presence of naked and enveloped intracellular capsids. Our previously described TCA precipitation assay monitors the incorporation of [^{3}H]thymidine-labeled DNA into capsids by measuring DNase I-resistant TCA-precipitable counts (22, 24) in whole-cell extracts and thus scores total packaged capsids. To measure the proportion of packaged capsids which are enveloped, we modified our conditions by digesting cell extracts with proteinase K prior to DNase I treatment and TCA precipitation. We reasoned that after proteinase K incubation, only enveloped virions would contain packaged, DNase I-resistant DNA.

To test the validity of these assays, the human hepatoma cell line HuH7 was infected at an MOI of 10 with HSV strain *ts*Prot.A, residual input virus was inactivated by an acid wash, and cells were incubated at 39°C in the presence of [^{3}H]thymidine (25 μCi/ml) to accumulate a population of immature procapsids. Cells were then downshifted to the permissive temperature of 31°C (after the addition of cycloheximide) for increasing amounts of time. Extracts were prepared and assayed for total packaged (Fig. 1A) and proteinase K-protected (enveloped) TCA-precipitable counts (Fig. 1B). As expected, at the end of the 39°C temperature block the levels of packaged and enveloped DNA were low. However, at successive times after the shift to 31°C, there was an increase in protected cpm as the population of immature capsids matured, initiated DNA packaging, and became enveloped. The increase was most rapid between 90 and 180 min downshift, with a subsequent slow increase observed over the next 13 h at 31°C.

If the envelopment assay truly measures the amount of packaged DNA enclosed by a lipid envelope then the signal should be abolished by the presence of detergent. Indeed, the addition of 0.05% Triton X-100 reduced the envelopment signal to background levels (Fig. 1B), but did not decrease the packaging signal (Fig. 1A). Some stimulation of the packaging signal was actually seen under these conditions, possibly due to an increase in efficacy of TCA precipitation in the presence of Triton X-100. The accumulation of mature infectious particles was confirmed by titrating each sample for PFU at successive time points of downshift to the permissive temperature (Fig. 1C). As expected, the kinetics of PFU production were similar to the rate of formation of enveloped particles. Thus, we have established simple, rapid and quantitative assays to measure both the total amount of DNase I-resistant TCA-precipitable viral DNA (termed the packaging signal) and proteinase K/DNase I-resistant viral DNA residing within lipid-bound capsids (termed the envelopment signal).

Biochemical detection of cytoplasmic virus particles. We next tested whether these assays could be used to examine those virus particles residing in the cytoplasm of HSV-infected cells. To do this, HuH7 cells were infected at an MOI of 10 with *ts*Prot.A and then incubated at 31°C for 16 h in the presence of [^{3}H]thymidine, and a PNS was prepared. Samples were subjected to density gradient ultracentrifugation on a 1.065-g/ml Percoll gradient, and fractions were collected from the top of the gradient. Each fraction was assayed for total packaged and enveloped DNA, and PFU were counted. As a control, we also subjected [^{3}H]thymidine-labeled extracellular secreted virus to similar centrifugation.

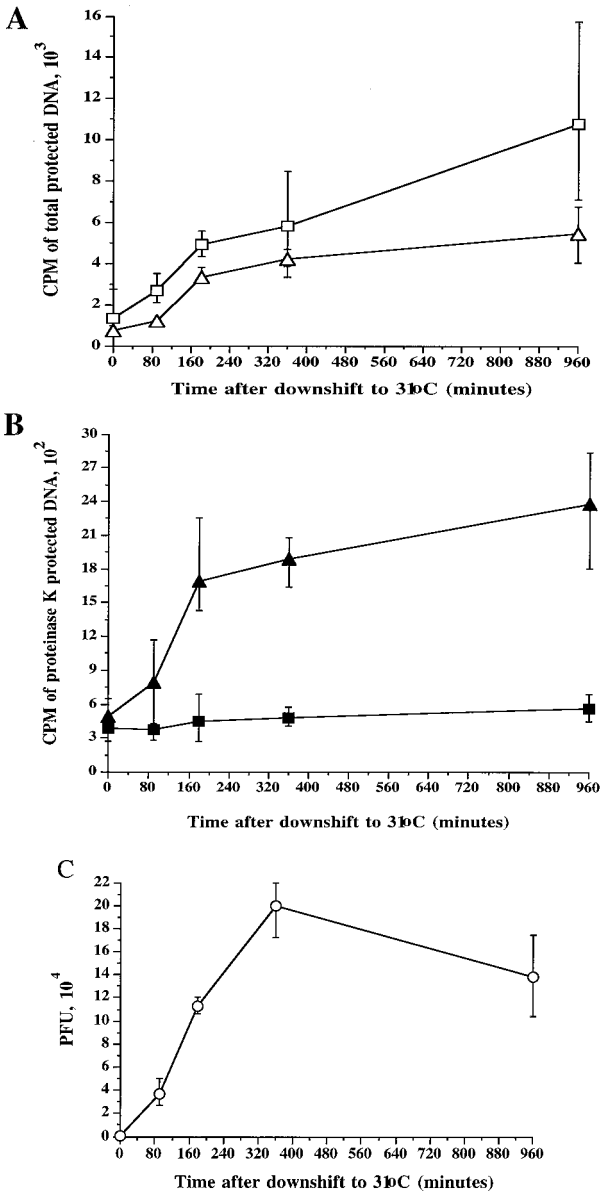

FIG. 1. Measuring DNA packaging and capsid envelopment using a TCA precipitation assay. HuH7 cells were infected with the HSV strain *ts*Prot.A, acid washed, and then incubated at 39°C in the presence of [^{3}H]thymidine. After 6.5 h, cycloheximide was added, and after a further 30 min the cells were downshifted to 31°C. Total cell extracts were prepared at particular times after downshift (indicated on the horizontal axes) and measured as follows. (A) DNase I-resistant (total packaged) DNA in the presence (squares) or absence (triangles) of 0.05% Triton X-100. (B) Proteinase K/DNase I-resistant (enveloped) DNA in the presence (solid squares) or absence (solid triangles) of 0.05% Triton X-100. (C) PFU present in each extract. In each case, plotted values represent the mean of two to four samples, and error bars indicate the range from the mean.

As can be seen in Fig. 2A, packaged and enveloped DNA present in extracellular, secreted virus particles sediments in a broad peak at the bottom of the gradient (fractions 12 to 20). The presence of mature enveloped virus in this region of the

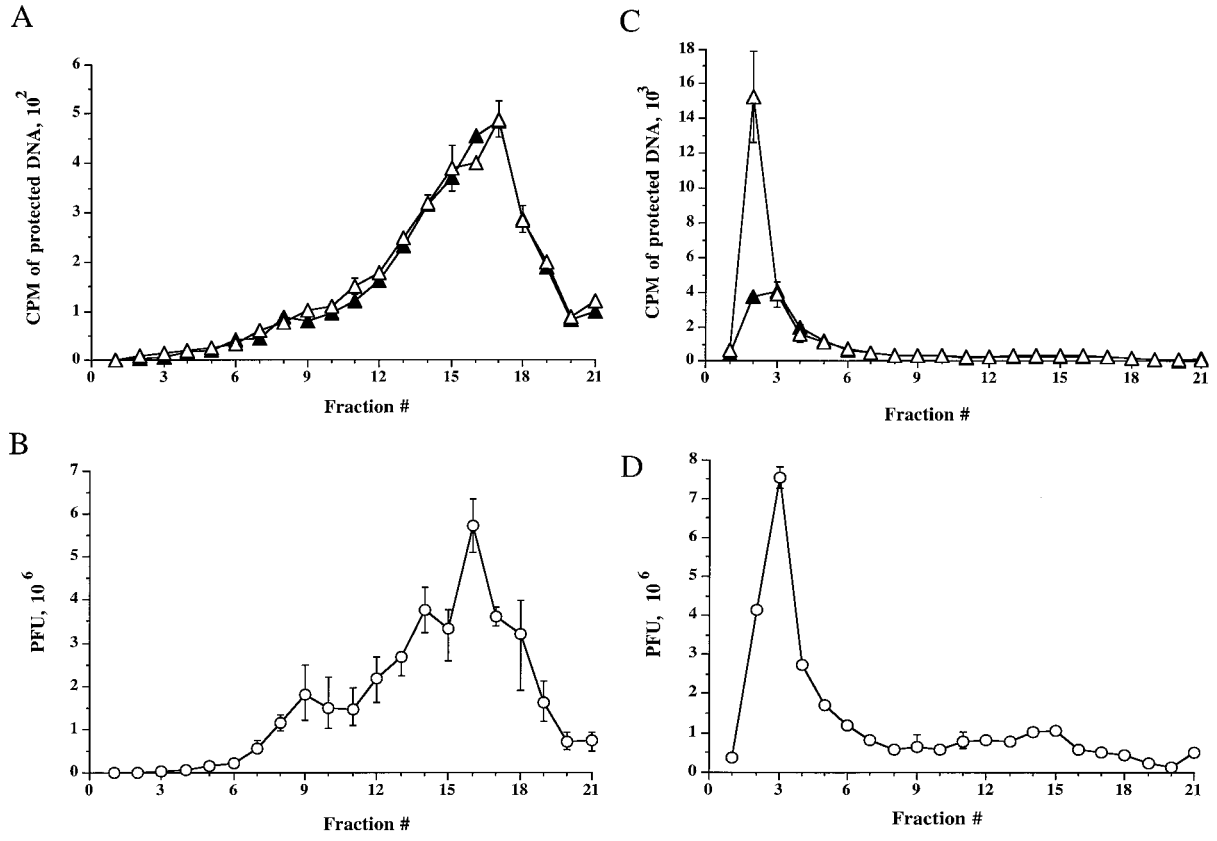

FIG. 2. Intracellular cytoplasmic virus is less dense than extracellular virus. [^{3}H]thymidine-labeled extracellular virus (A and B) or PNS intracellular virus (C and D) from *ts*Prot.A-infected HuH7 cells were subjected to isopycnic centrifugation on a 1.065-g/ml self-forming Percoll gradient. Gradients were fractionated from the top (corresponding to fraction 1), as indicated on the horizontal axes. (A and C) Fractions were assayed for total packaged DNA (open triangles) or proteinase K-protected, enveloped DNA (solid triangles). (B and D) Fractions were titrated for PFU (open circles). Plotted values represent the means of duplicate samples, and error bars indicate the range from the mean.

gradient was further confirmed by PFU analysis across these fractions (Fig. 2B). The density of this peak is in general agreement with that reported for enveloped HSV particles, 1.09 to 1.11 g/ml (74, 75). The total packaged DNA signal was equivalent to the envelopment signal, consistent with the expectation that all extracellular mature virions should be completely enveloped. This also implies that enveloped virus particles are not mechanically disrupted during the ultracentrifugation procedure.

Strikingly, the sedimentation profile for intracellular virus was very different. Intracellular virus was present at a much lighter buoyant density (fractions 2 to 5) than extracellular particles (fractions 12 to 20), defined by TCA-precipitable counts and PFU numbers, as shown in Fig. 2C and 2D, respectively. The simplest explanation for this is that the HSV particles are contained within or associated with low-buoyant-density cytoplasmic organelles. It is also interesting that when every gradient fraction is taken into account, the cpm derived from enveloped capsids is only 58% of that obtained from total capsids, suggesting that these intracellular virus particles consist of both naked and enveloped capsids, in contrast to that observed for extracellular virions. This was unexpected, since nonenveloped capsids would be expected to sediment at the bottom of the gradient with a density of 1.13 to 1.15 g/ml under these conditions (74, 75). We hypothesized that low-density naked capsids might result from tethering of capsids to the cytoplasmic face of a low-density organelle, and electron microscopic inspection subsequently yielded data consistent with this possibility (see Fig. 4). Since all extracellular particles appear to be fully enveloped under these conditions, and since the ratio of naked to enveloped capsids in the starting PNS is similar to that after density gradient centrifugation (data not shown), it is unlikely that the presence of unenveloped capsids in these light gradient fractions is an artifact of organelle breakage during centrifugation.

To identify the intracellular compartment in which virus particles reside, we subjected each gradient fraction to Western blot analysis and marker enzyme assay. The lysosomal compartment, detected by acid phosphatase activity, was found to sediment at the bottom of the gradient (fractions 18 to 21), consistent with previously published observations (33). However, all other organelle markers cofractionated with intracellular virus at the top of the gradient, making this gradient system unsuitable for further organelle characterization (data not shown).

Cytoplasmic virus cofractionates with Golgi and endosomal markers. To further analyze the subcellular distribution of HSV, radiolabeled intracellular and extracellular virus were

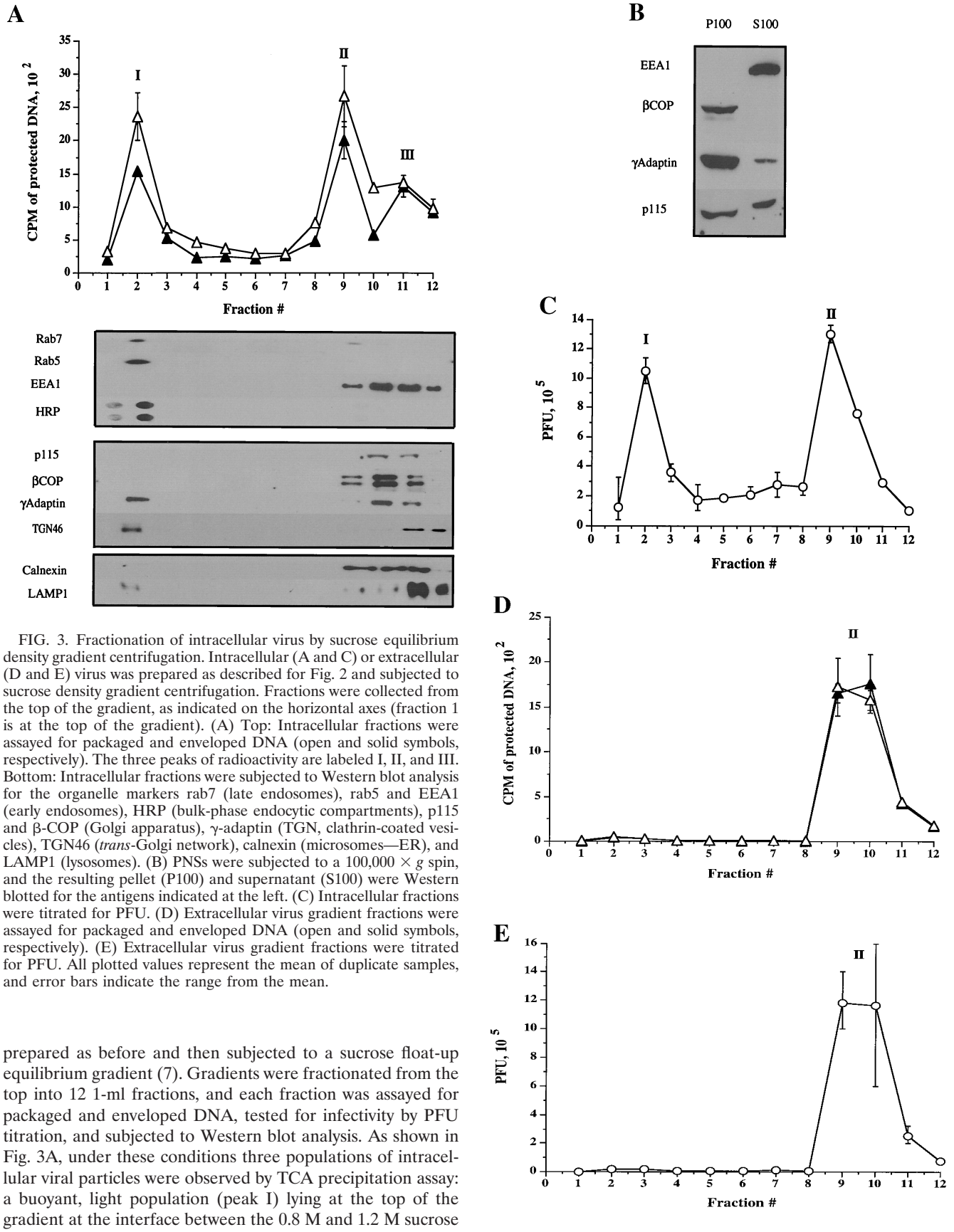

FIG. 3. Fractionation of intracellular virus by sucrose equilibrium density gradient centrifugation. Intracellular (A and C) or extracellular (D and E) virus was prepared as described for Fig. 2 and subjected to sucrose density gradient centrifugation. Fractions were collected from the top of the gradient, as indicated on the horizontal axes (fraction 1 is at the top of the gradient). (A) Top: Intracellular fractions were assayed for packaged and enveloped DNA (open and solid symbols, respectively). The three peaks of radioactivity are labeled I, II, and III. Bottom: Intracellular fractions were subjected to Western blot analysis for the organelle markers rab7 (late endosomes), rab5 and EEA1 (early endosomes), HRP (bulk-phase endocytic compartments), p115 and β-COP (Golgi apparatus), γ-adaptin (TGN, clathrin-coated vesicles), TGN46 (*trans*-Golgi network), calnexin (microsomes—ER), and LAMP1 (lysosomes). (B) PNSs were subjected to a 100,000 × *g* spin, and the resulting pellet (P100) and supernatant (S100) were Western blotted for the antigens indicated at the left. (C) Intracellular fractions were titrated for PFU. (D) Extracellular virus gradient fractions were assayed for packaged and enveloped DNA (open and solid symbols, respectively). (E) Extracellular virus gradient fractions were titrated for PFU. All plotted values represent the mean of duplicate samples, and error bars indicate the range from the mean.

prepared as before and then subjected to a sucrose float-up equilibrium gradient (7). Gradients were fractionated from the top into 12 1-ml fractions, and each fraction was assayed for packaged and enveloped DNA, tested for infectivity by PFU titration, and subjected to Western blot analysis. As shown in Fig. 3A, under these conditions three populations of intracellular viral particles were observed by TCA precipitation assay: a buoyant, light population (peak I) lying at the top of the gradient at the interface between the 0.8 M and 1.2 M sucrose layers in fraction 2, and two denser populations of virus (peaks

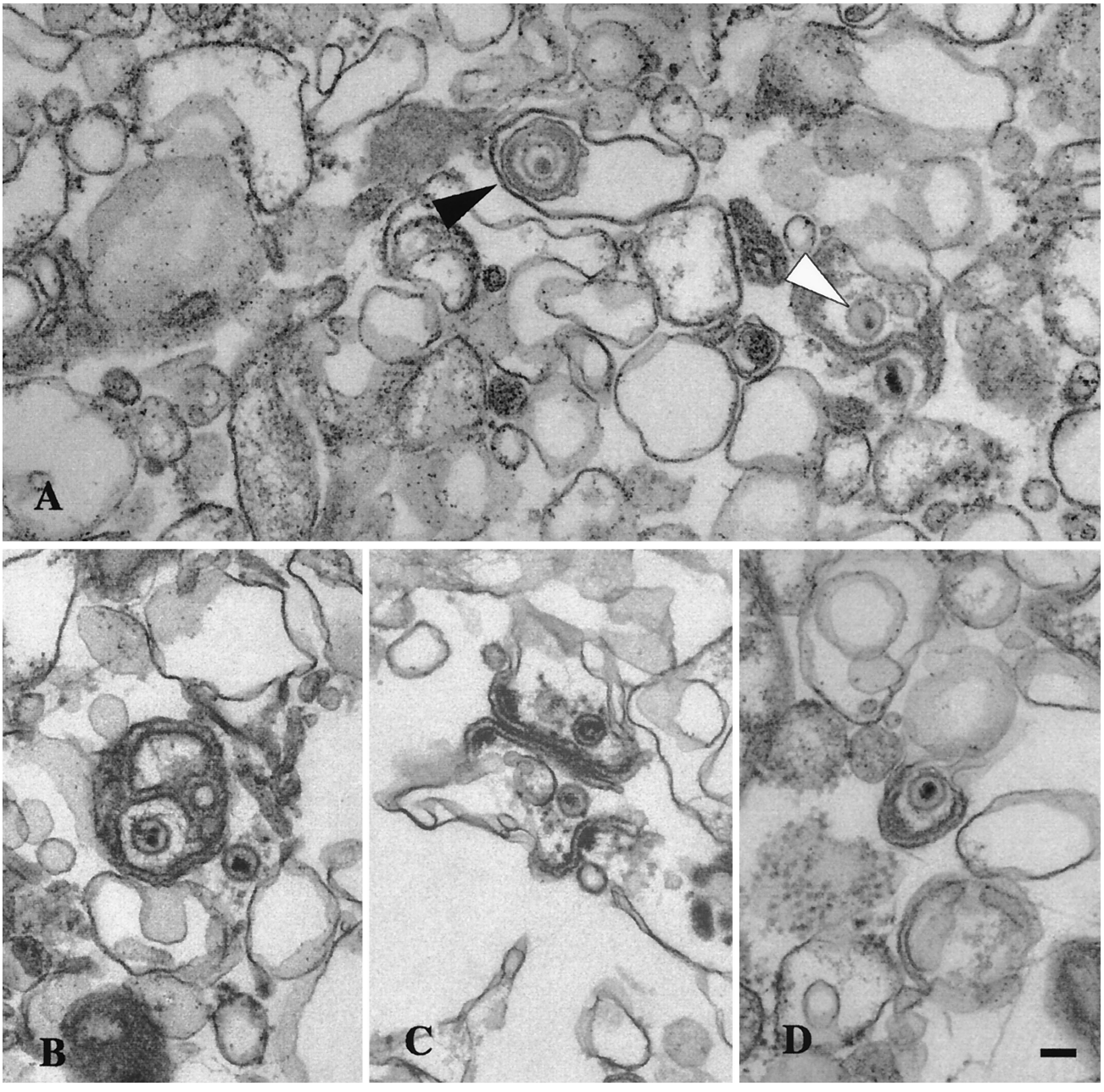

FIG. 4. Ultrastructural analysis of peak I. Material from peak I was pelleted and fixed in glutaraldehyde and prepared for transmission electron microscopy as described in the text. (A) Enveloped virus particle enclosed within a smooth membrane compartment (indicated by the black arrow head) and naked capsids in close proximity to an organellar membrane (indicated by the white arrowhead). (B, C, and D) Additional representative images from peak I. Bar, 0.1 μm.

II and III) within the 1.4 M and 2.0 M sucrose layers, in fractions 9 and 11-12, respectively. As previously observed for intracellular virus, the cpm derived from packaged capsids is greater than that for enveloped capsids (Fig. 3A, peaks I and II). Interestingly, although all three peaks appear to contain enveloped virus (Fig. 3A), PFU were only present in peak I and peak II, not in peak III (Fig. 3C). When every gradient fraction was taken into account, 72% of the total capsid population was enveloped under these conditions.

In contrast to intracellular virions, density gradient fractionation of extracellular virus resulted in a single peak of TCA-precipitable material and PFU in the same location as peak II (Fig. 3D and E), and, as expected for secreted virions, equivalent packaged and enveloped signals were obtained. The similarity in density between intracellular peak II particles and extracellular virus led us to suspect that peak II may represent enveloped particles released from intracellular organelles due to their breakage upon gradient centrifugation. Consistent with this, such viral particles were only observed in sucrose float-up gradients (which require 4 h of centrifugation and are

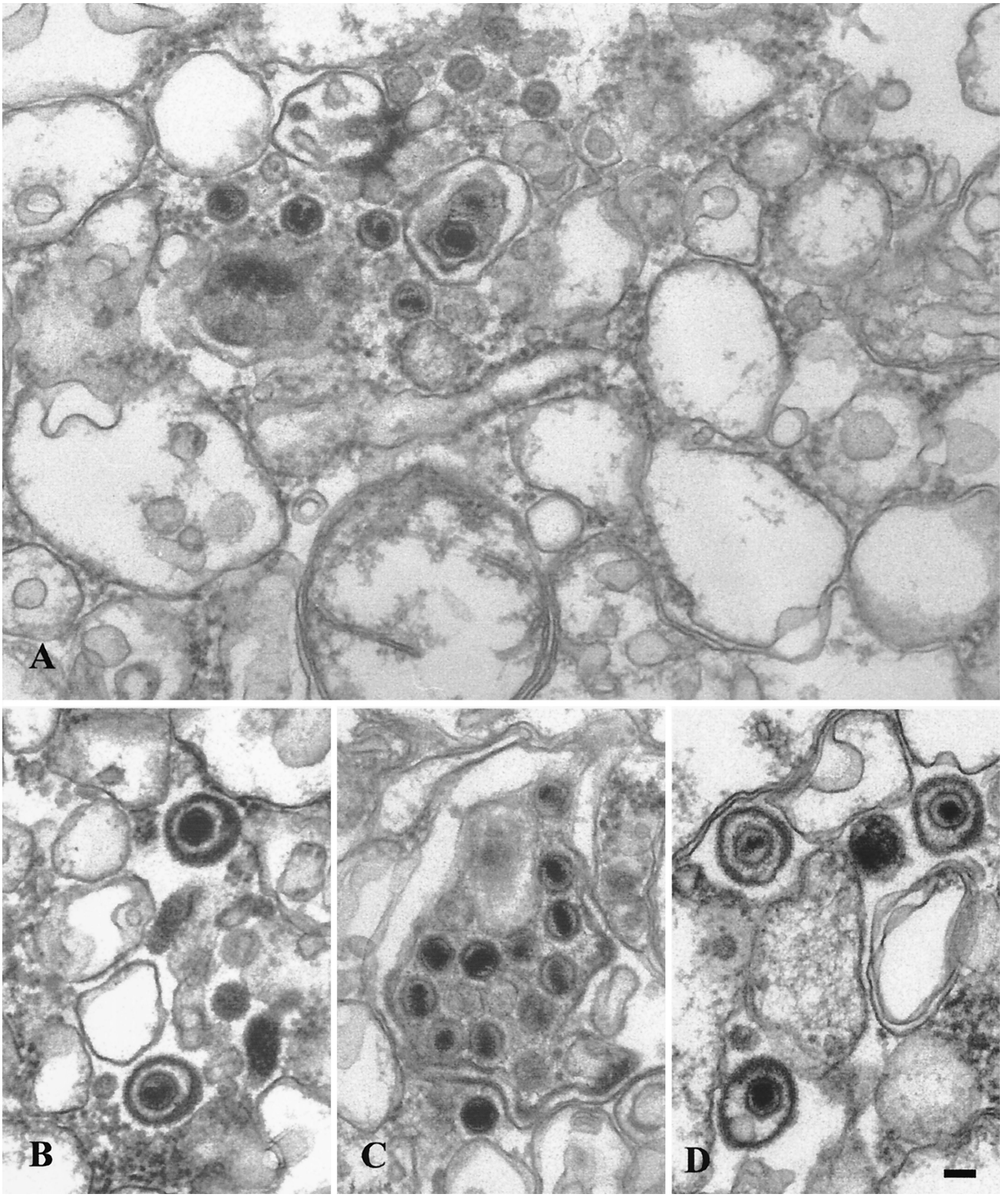

FIG. 5. Ultrastructural analysis of peak II. Extracts were prepared as described for Fig. 4. (A) Representative section showing mainly naked capsids. (B and D) Presence of singularly enveloped virus particles and (C) a cluster of capsids enclosed within a single membrane, a minor population in this fraction. Bar, 0.1 μm.

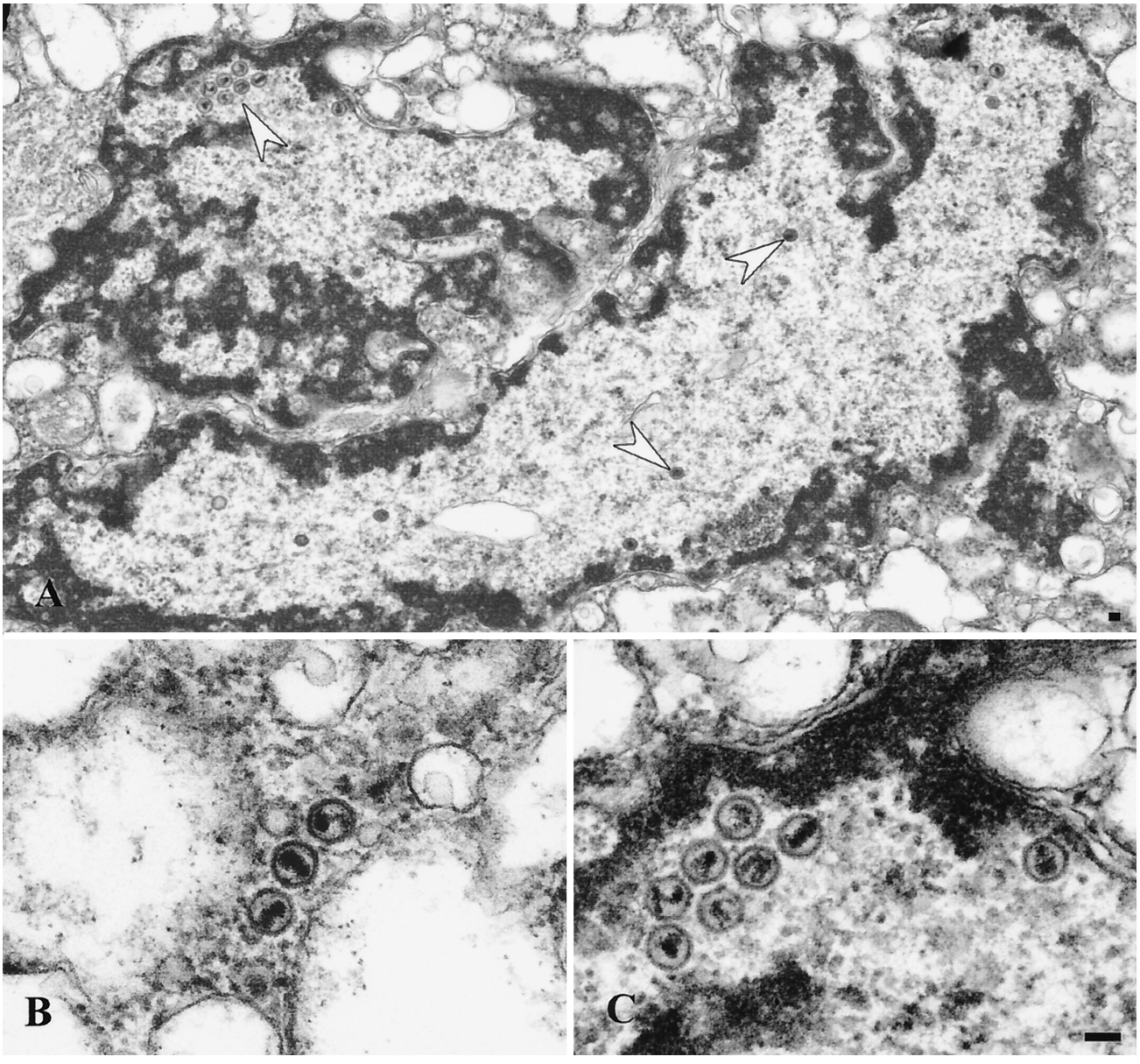

FIG. 6. Ultrastructural analysis of peak III material. Extracts were prepared as for Fig. 4. (A) Nuclear fragment containing clusters of naked capsids or single capsids (indicated by the white arrows). The region in the upper left, indicated by an arrow, is magnified in panel C. (B) Free naked capsids. Bar, 0.1 μm.

loaded under nonisoosmotic conditions) and were never seen following Percoll gradient fractionation (Fig. 2), which is isoosmotic and complete in 45 min. Furthermore, electron microscopic analysis confirmed that peak II contained enveloped virions not bound by an organellar membrane (see Fig. 5). The location of peak III on gradient centrifugation implies that peak III may represent capsids associated with large, dense structures, which was subsequently confirmed by electron microscopic analysis (see Fig. 6). Although this distribution of virions was observed using *ts*Prot.A-infected HuH7 cells grown at 31°C, similar results were observed following infection of COS cells at 37°C with the wild-type HSV strain SC16 (data not shown).

To determine the distribution of cytoplasmic organelles within the sucrose density gradient, fractions were subjected to Western blot analysis (lower part of Fig. 3A). Peak I is highly enriched in Golgi apparatus, TGN, endosomes, and associated vesicles, as shown by the presence of the endosomal markers rab5 and rab7 (18, 50), the TGN marker TGN46 (56), γ-adaptin (60), and enzymes of the *trans*-Golgi, galactosyltransferase and sialyltransferase (shown in Fig. 8, below). The presence of the endocytic network in this part of the gradient was also demonstrated by allowing cells to endocytose HRP from the medium prior to PNS preparation. As can be see in Fig. 3A, HRP accumulated exclusively in peak I, as shown by direct chemiluminescence detection.

Other organellar markers were found in the denser fractions of the gradient, corresponding to the peak II and III virus

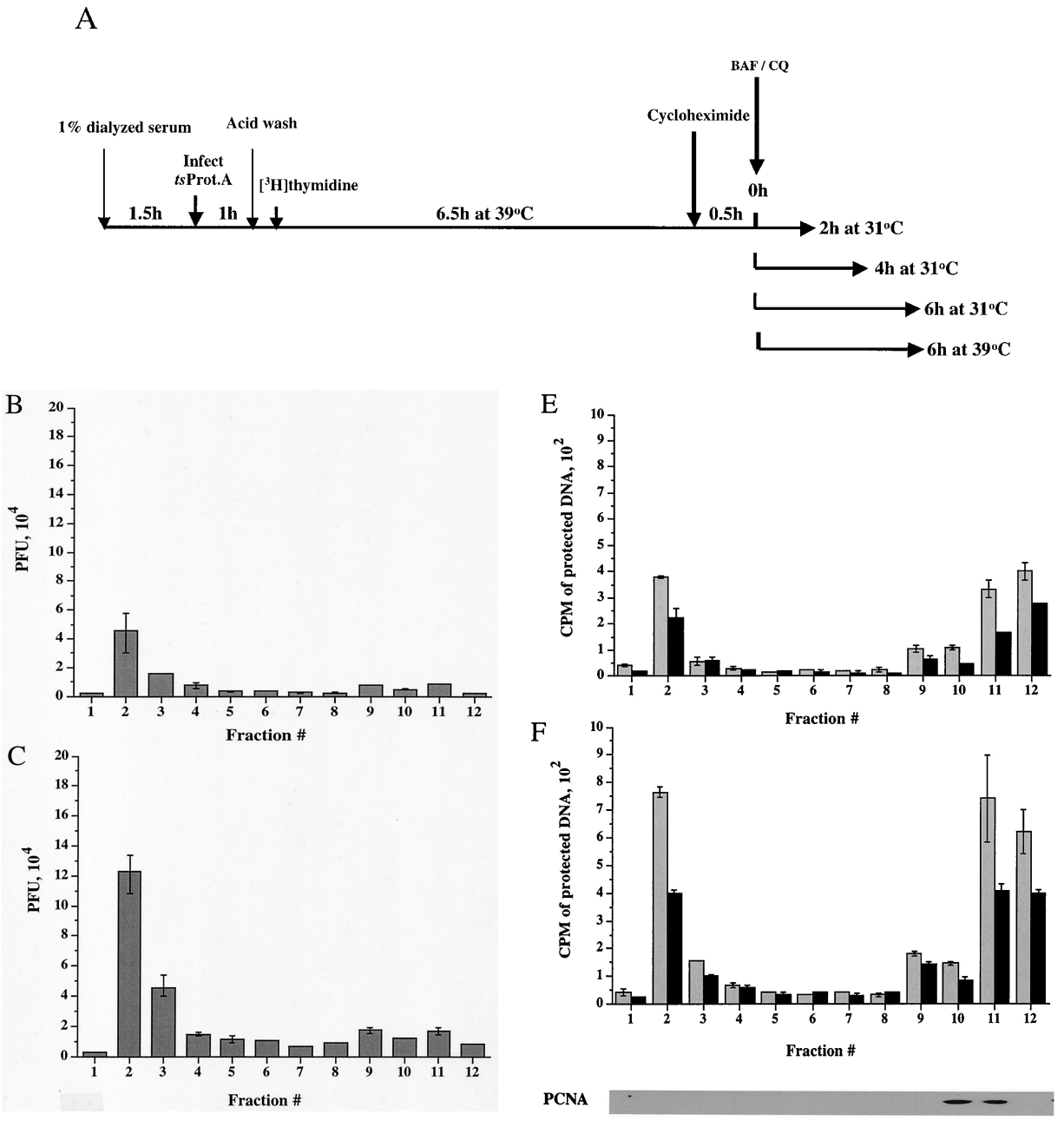

FIG. 7. Time course of delivery of virus to cytoplasmic organelles. (A) Schematic showing the time course and conditions for this experiment. HuH7 cells were infected with *ts*Prot.A and incubated for 7 h at 39°C in the presence of [^{3}H]thymidine (cycloheximide was added 30 min prior to downshift). Cells were downshifted to 31°C for 0, 2, 4, or 6 h or kept at 39°C for a further 6 h. For each time point, a PNS was prepared and subjected to sucrose gradient centrifugation, and fractions were titrated for PFU. BAF/CQ indicates the time of addition of the drugs bafilomycin A1 and chloroquine in the experiments shown in Fig. 9. (B to D) PFU yields 2, 4 and 6 h after downshift, respectively. Fractions were also assayed for total packaged DNA (light bars) and enveloped DNA (dark bars) at 2, 4, 6, and 0 h after downshift to 31°C (panels E to H, respectively) or after an additional 6 h at 39°C (panel I). Plotted values are means of duplicates, and error bars indicate the range from the mean. An immunoblot for a nuclear marker, proliferating cell nuclear antigen (PCNA), was performed on fractions from a representative 4-h-downshifted gradient (F).

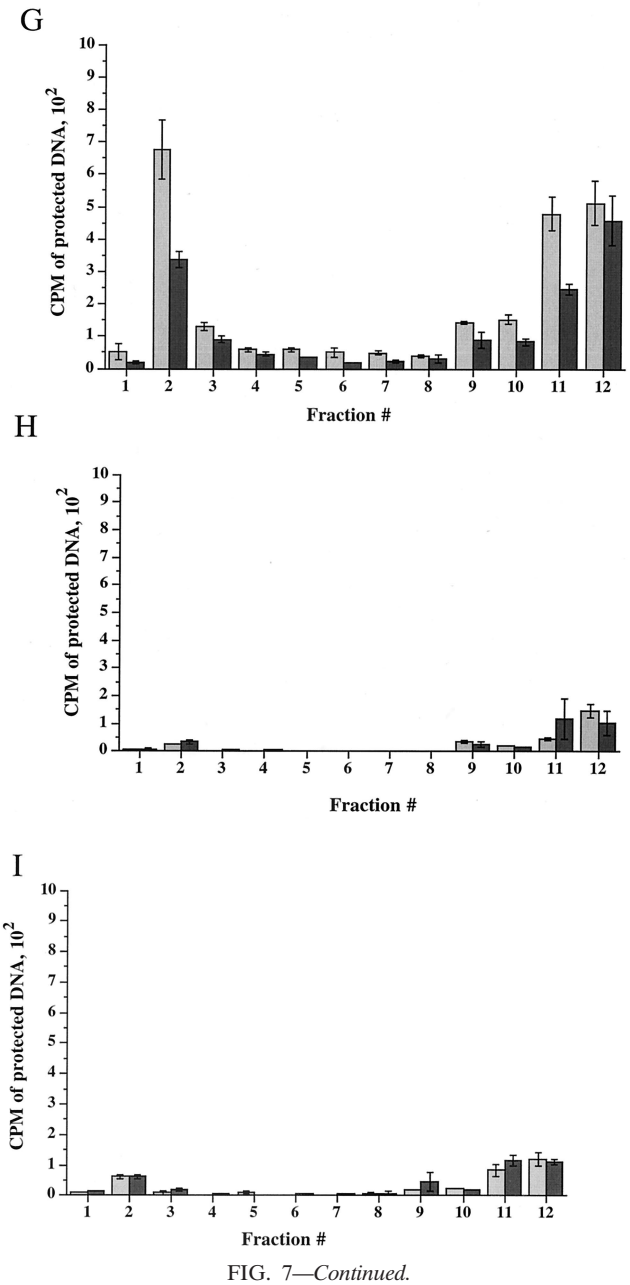

FIG. 7—*Continued.*

populations, as shown by the distribution of calnexin (ER) and LAMP1 (lysosomes) (61, 73). Surprisingly, the peripheral early endosomal marker EEA1 (52) and the peripheral Golgi proteins βCOP (31) and p115 (77) also remained at the bottom of the gradient. Following centrifugation of a PNS at 100,000 × *g* (Fig. 3B), EEA1 was found to be exclusively cytoplasmic under our conditions, unlike the endosomal marker rab5. In HSV-infected HuH7 cells, this antigen therefore cannot be used to determine the distribution of early endosomes. All of the βCOP and a substantial portion of p115 were found to be membrane associated in the PNS (Fig. 3B), despite the fact that they did not float with the Golgi glycosyltransferase activities to peak I (shown in Fig. 8 below). The most likely explanation for this is that these peripheral proteins dissociate from the surface of the Golgi cisternae during sucrose gradient centrifugation.

Since peak I contains endosomes, we were concerned that virions in this fraction may represent particles that had already been secreted and were subsequently re-endocytosed. To address this concern, we infected HuH7 cells with *ts*Prot.A at an MOI of 10, and the infection was allowed to proceed for 11 h in the absence of radiolabel. Purified, secreted [^{3}H]thymidine-labeled HSV was then added to the culture medium for 2 or 5 h at 31°C to allow its possible endocytosis, and cell extracts were prepared and loaded onto a sucrose equilibrium gradient. No TCA-precipitable DNA was present in any gradient fraction (data not shown), suggesting that under our assay conditions, any secreted virus which had been reendocytosed was undetectable.

Ultrastructural features of gradient fractions from *ts*Prot.A-infected cells. To further investigate the nature of virus particles in peaks I, II, and III, a sample of each was subjected to transmission electron microscopy. Consistent with our previous biochemical data, peak I was found to contain enveloped virions fully enclosed by a smooth membrane and also naked capsids in close proximity, and presumably attached, to these organelles (Fig. 4). Interestingly, an electron-dense tegument-like material can often be observed at the surface of these membranes and between the capsid and the bilayer. These structures are similar to those observed in infected cell cytoplasms and are interpreted to represent capsids either budding into or erroneously emerging from cellular organelles (14, 27). Analysis of peak II material revealed the presence of both naked capsids and singularly enveloped virus particles, as shown in Fig. 5. These structures are entirely consistent with the biochemical observation that mature extracellular virus fractionated at this position upon gradient centrifugation, and peak II virions therefore most likely represent enveloped capsids released from broken peak I organelles. We also observed, at lower frequency, aberrant multicapsid clusters surrounded by a single membrane bilayer (Fig. 5C). Analysis of peak III material revealed the presence of naked capsids (Fig. 6B) or large membrane-bound structures which contain chromatin-like electron-dense material and single or clustered capsids (Fig. 6A and C) and which appear to be fragments of cells and nuclei. The presence of capsids within nuclear fragments explains why our biochemical assays detected an apparent envelopment signal in peak III despite the absence of infectivity (Fig. 3A and C).

In summary, the three gradient peaks contain structures consistent with the results of our biochemical and PFU analyses. We have not attempted a quantitative ultrastructural analysis of the organelles visible in these virus-containing fractions and therefore draw no morphology-based conclusions about the identity of the HSV-associated organelles present in Fig. 4 to 6.

Kinetics of viral egress. To further test the relationship between peak I and peak II, we determined the kinetics of delivery of viral particles to cytoplasmic compartments during a synchronous wave of viral egress. The experimental approach is outlined in Fig. 7A. HuH7 cells were infected at an MOI of 10 for 1 h at 37°C with HSV strain *ts*Prot.A, the residual input virus was removed by acid wash, and cells were incubated at 39°C for 7 h. At 30 min prior to downshift, cycloheximide was

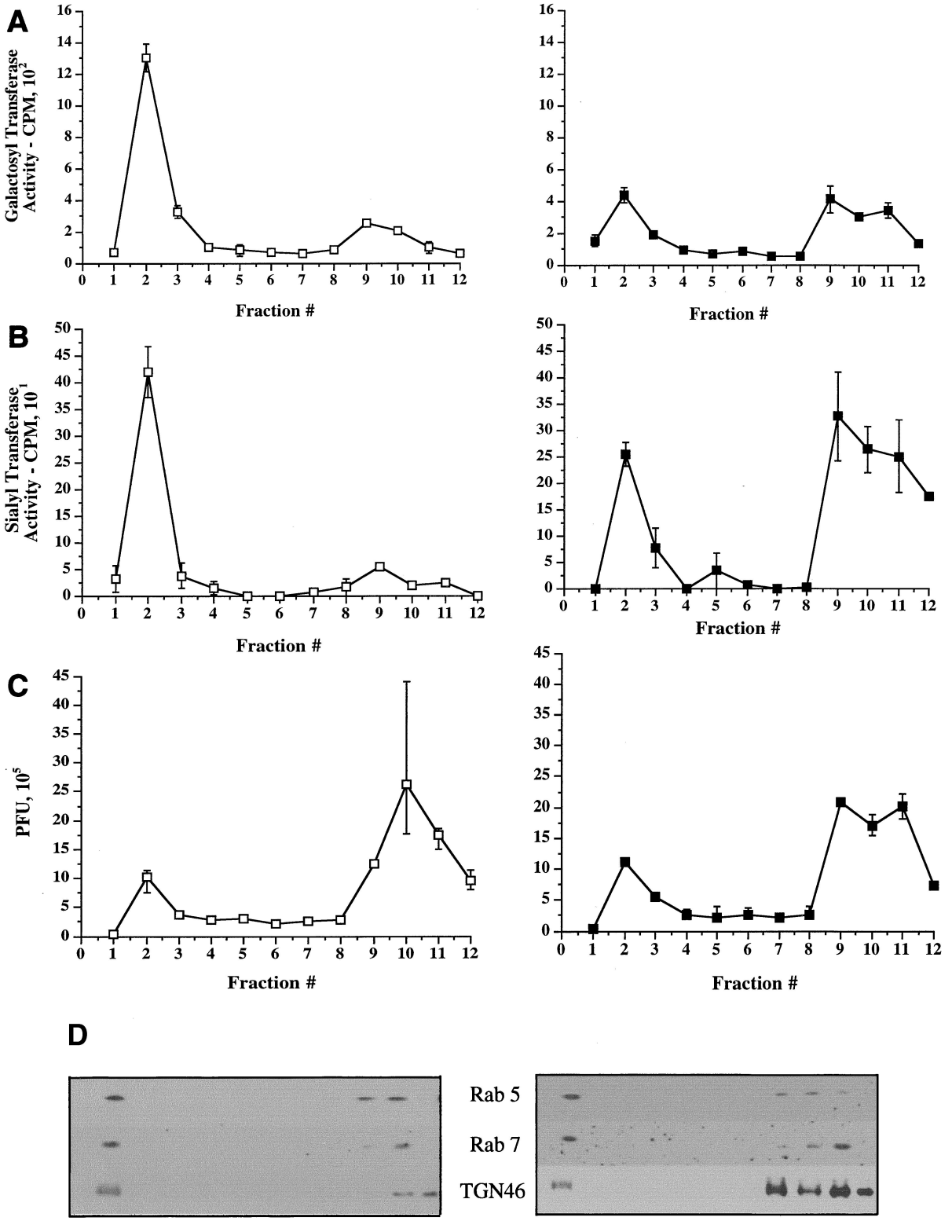

added, and the cells were downshifted to 31°C for 0, 2, 4, and 6 h or maintained at 39°C for a further 6 h. At each time point, PNSs were collected and subjected to sucrose gradient centrifugation. Each fraction was also titrated for infectivity.

We reasoned that after short periods at 31°C, we would observe the initial organelle into which virus is delivered following exit from the nucleus. Indeed, after 2 h at 31°C, infectious virus, as measured by PFU, was primarily present in peak

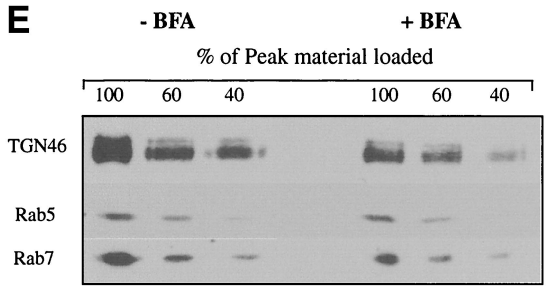

FIG. 8. Use of BFA to separate Golgi cisternae from TGN/endosomes. An experiment similar to that in Fig. 3 was performed, except that cells were incubated with BFA (5 μg/ml) prepared in ethanol (righthand panels, solid symbols) or with an equivalent volume of ethanol alone (lefthand panels, open symbols) for 1 h prior to PNS preparation and fractionation. Fractions were assayed for galactosyltransferase activity (A), sialyltransferase activity (B), or PFU (C) or Western blotted for rab5, rab7, and TGN46 (D). (E) Peak I was collected following fractionation of BFA-treated and mock-treated cells (as indicated) and then Western blotted as in panel D. Lanes contained 100, 60, or 40% (as indicated at the top of the figure) of the peak I material in panel D.

I (Fig. 7B). As incubation at 31°C continued for 4 or 6 h, there was a continuous delivery of PFU specifically to peak I (Fig. 7C and D), with little accumulation in peak II. These data suggest that under our conditions, most mature infectious virus is first observed within peak I organelles after exit from the nucleus.

When packaging and envelopment assays were performed on these fractions (Fig. 7E to I), signals were found within peak I, as expected from our PFU analysis. However, there was also an unexpectedly high signal in peak III (shown above to represent nucleus-associated capsids), much greater than in a steady-state infection (compare Fig. 7G with Fig. 3A). It has previously been reported that the addition of cycloheximide during an HSV infection induces apoptosis (44), with infected cells showing perinuclear chromatin condensation and nuclear fragmentation. The increased accumulation of nucleus-derived debris in peak III is therefore most likely due to the presence of cycloheximide during the downshift to 31°C. Consistent with these conclusions and our electron microscopic data, Western blotting showed that peak III contains the nuclear marker protein proliferating cell nuclear antigen (PCNA) (40), as shown in Fig. 7F.

The lack of both PFU and TCA-precipitable cpm at the position of peak II following downshift may be because organelles are more stable at this early time of infection and do not break on sucrose gradient fractionation. Indeed, at longer times post downshift, some peak II virus did accumulate (see Fig. 9). No packaging or envelopment was observed in fractionated PNS prepared from cells collected immediately following the shift to 31°C or maintained at the nonpermissive temperature of 39°C (Fig. 7H and I). Taken together, our PFU analysis and packaging/envelopment data suggest that under these assay conditions, during a synchronous wave of virus exit, HSV particles are initially targeted to the organelles present in peak I.

Separation of Golgi from TGN and endosomes using brefeldin A. From the data in Fig. 3A, peak I appears to contain markers characteristic of endosomes (rab5 and rab7) and is the exclusive site of accumulation of a bulk-phase endocytic marker (exogenously added HRP). However, it also contains the TGN markers γ-adaptin and TGN46 and (as shown in Fig. 8 below) glycosyltransferase activities characteristic of the *trans*-Golgi cisternae. We attempted a number of density gradient centrifugation techniques to separate these organelles and to determine which compartments contain infectious HSV, but were unsuccessful. We therefore chose to exploit the properties of the drug brefeldin A (BFA). BFA addition is known to cause disassembly of the *cis*-, *medial*-, and *trans*-Golgi cisternae and their fusion with the ER. In contrast, the TGN appears to fuse and mix with the endocytic network (47, 81). This enables density gradient separation of the TGN and the endosomal apparatus from Golgi, since fusion of Golgi with the ribosome-studded ER greatly increases the density of Golgi-derived membranes.

HuH7 cells were infected with *ts*Prot.A and incubated at 31°C for 16 h, and a PNS was prepared and fractionated exactly as in Fig. 3 except that BFA was added or omitted 1 h before the end of the incubation. Note that these are very short BFA incubations and thus differ markedly from experiments which studied the long-term effect of BFA treatment on the overall process of HSV replication (20). Fractions were assayed for PFU and the *trans*-cisternal markers sialyltransferase and galactosyltransferase and Western blotted for TGN46 and the endosomal antigens rab5 and rab7. As shown in Fig. 8, in untreated samples *trans*-Golgi glycosyltransferases, TGN46, and endosomes floated to peak I. However, the distribution was quite different following fractionation of BFA-treated cells. BFA treatment resulted in approximately 40 to 70% of the *trans*-Golgi glycosyltransferases shifting to the load region of the gradient due to mixing of Golgi cisternae with dense microsomes, as previously demonstrated (67, 68). We have not tested markers of the *medial* and *cis* compartments of the Golgi apparatus, but despite extensive studies of the effects of BFA, the drug has never been observed to fuse *trans* cisternae with the ER without also redistributing earlier cisternae.

In contrast to the effect on Golgi cisternae, there was no apparent redistribution of the TGN/endosomal markers TGN46, rab5, and rab7, as expected (Fig. 8D). Figure 8E shows that if two thirds or more of the TGN/endosomes actually had shifted out of peak I, we would have been able to observe this by Western blot under these conditions. In the study shown in Fig. 8, TGN46 showed some variation in distribution and intensity in the load region of these gradients (consider fractions 9 to 12 in Fig. 8D). The reasons for this are unclear, but the magnitude of the effect was not reproducible and in repeat studies was always less than shown in Fig. 8D. Despite this observation, there was no apparent change in the intensity of TGN46 in peak I, so we conclude that little or no TGN was lost from this region of the gradient.

Having confirmed that Golgi cisternae but not TGN/endosomes had been depleted from peak I, we tested the distribution of infectious HSV particles under these conditions. Strikingly, BFA treatment had no effect on the number of infectious particles in peak I, and the distribution of PFU was identical in drug-treated and control cells (Fig. 8C). These data are consistent with HSV localization to the TGN/endocytic compartment rather than to the cisternae of the Golgi apparatus.

Neutralization of organellar pH. The TGN and endosomes are known to maintain a low internal pH (between approxi-

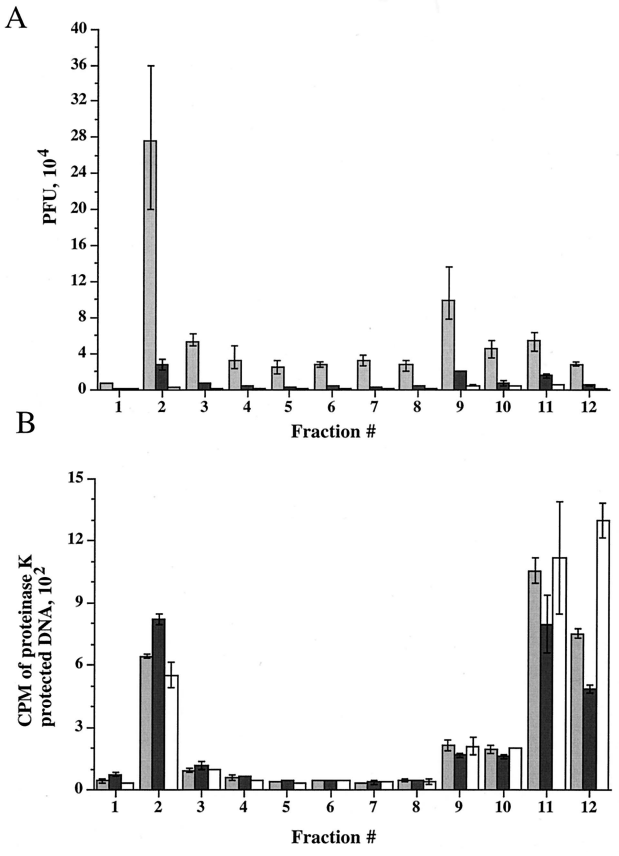

FIG. 9. Infectivity of virus particles within cytoplasmic organelles is dependent on an acidic environment. HuH7 cells were infected with the HSV-1 strain *ts*Prot.A, acid washed, and then incubated at 39°C for 7 h. Cycloheximide (20 μg/ml) was added 30 min prior to downshift to 31°C. At the time of downshift, cells received 150 μM chloroquine or 200 nM bafilomycin A1 or no treatment as shown in Fig. 7A. Cells were then incubated at 31°C for 9 h. PNSs were subjected to sucrose gradient centrifugation and fractionated. (A) PFU titrations of gradient fractions from untreated cells (light gray bars) and cells treated with chloroquine (dark gray bars) or bafilomycin A1 (open bars). (B) Assay for enveloped virions present in untreated cells and cells treated with chloroquine or bafilomycin A1 (indicated as in A). All values plotted are means of duplicate samples, and error bars indicate the range from the mean.

mately 5 and 6.5), which is required for their normal biological function. If these organelles truly play a critical role in HSV assembly and egress, then we reasoned that these processes might be interrupted by addition of the weak base chloroquine (17) or the drug bafilomycin A1, which inhibits the proton ATPase responsible for acidification (2, 6, 10, 82, 83).

To test whether chloroquine or bafilomycin A1 could render organelles unable to support virus assembly, HuH7 cells were infected with *ts*Prot.A for 7 h at 39°C and then downshifted to 31°C for 9 h in the presence of cycloheximide (20 μg/ml) and either 150 μM chloroquine or 200 nM bafilomycin A1, as shown in Fig. 7A. Extracts were subjected to gradient density centrifugation, and each fraction was assayed for PFU or measured for TCA-precipitable counts (Fig. 9). Note that in these studies prolonged incubation at 31°C resulted in the appearance of a small virus signal in peak II, consistent with our suggestion that this material is derived from unstable organelles breaking during centrifugation. Interestingly, PFU in peak I decreased 10-fold following incubation with chloroquine and more than 130-fold after treatment of cells with bafilomycin A1 (Fig. 9A). Furthermore, peak II virus infectivity was also diminished, as would be expected if the particles were derived from peak I.

Since the recovery of organelle-associated infectious particles was dramatically reduced in chloroquine- and bafilomycin A_1-treated cells, we tested whether the accumulation of enveloped particles within peak I was affected. Surprisingly, upon gradient centrifugation of these extracts, no significant difference in the envelopment signal across the gradient was observed (Fig. 9B). Thus, although PFU production was abolished within chloroquine- and bafilomycin A_1-treated cells, formation of cytoplasmic enveloped particles appears unaffected. Electron microscopic analysis revealed no gross structural differences between peak I HSV particles prepared from control and bafilomycin A1-treated cells (data not shown).

DISCUSSION

A major challenge in the study of HSV-1 egress from infected cells has been the interpretation of electron microscopic images showing cytoplasmic virus adjacent to or within membranous organelles. The relevance of these various structures to assembly and exocytosis of infectious HSV particles has been much discussed, and several hypotheses have been suggested to explain their role and origin (27). In this study we describe a biochemical approach to the analysis of HSV egress. We have developed rapid and quantitative assays which enable us to measure naked and enveloped capsids as they travel through the cytoplasm of infected cells. Using these assays and differential centrifugation techniques, we have isolated a gradient fraction which contains infectious HSV and markers characteristic of the Golgi apparatus, TGN, and endosomes. Addition of the drug BFA enabled further subdivision of this fraction, resulting in removal of the majority of the *trans*-Golgi (and, by implication, the entire Golgi stack) but leaving behind TGN, endosomes, and all of the PFU. The simplest interpretation of these data is that the HSV particles are present within the lumen of the TGN and/or endocytic network, which in the latter case includes early and late endosomes, and sorting endosomes (50). We cannot discount the possibility that BFA caused disassembly of the *trans*-Golgi cisternae without affecting the *cis* or *medial* compartments and that the PFU in peak I reside exclusively in these BFA-resistant cisternae, bypassing the *trans* cisternae as they traffic out of the cell. However, selective BFA resistance of cisternae and bypass of the *trans*-Golgi during trafficking are without precedent, and it is difficult to imagine a mechanism by which such phenomena could occur.

Consistent with a role for TGN and/or the endocytic apparatus in HSV assembly is the effect of organellar pH neutralization. Previous work has shown that the weak bases NH_4Cl and chloroquine inhibit production of infectious HSV particles (5, 42, 43, 45, 46), but in those studies the bases were usually present throughout the infection and could have affected any step in replication. We showed that chloroquine and bafilomycin A1 (a specific drug which blocks endosomal acidification) abolish infectivity in peak I when added after accumulation of

synchronized *ts*Prot.A procapsids. These compounds must therefore inhibit some step after procapsid assembly. Consistent with this notion, normal numbers of enveloped though noninfectious particles were found within neutralized organelles. Interestingly, addition of monensin to HSV-infected cells, which would also result in pH neutralization (8, 26), led to accumulation of infectious virions (38), though at diminished levels compared to controls. However, those studies considered PFU in total cell extracts (presumably including any infectious virions in the perinuclear space) rather than the neutralized organelle itself.

Peak I was the only detectable destination for exocytosing virions during the earliest stages of a controlled wave of *ts*Prot.A assembly. PFU reached the organelles in this region of the gradient within 2 h of the start of procapsid maturation; however, these studies were conducted at 31°C, and the rate at 37°C might well be higher (and this 2-h time period includes the time required for capsid maturation and DNA packaging, shown to be 40 to 60 min in our earlier studies [23]). Under these conditions, PFU were not detectable in the medium until 4 h after it was first observed in peak I (data not shown). This suggests that exit of HSV from this compartment is slow at 31°C and also shows that TGN/endosomes are unlikely to contain HSV as a result of having endocytosed it from the medium (consistent with the fact that exogenously added radiolabeled HSV was not detectable in peak I under our conditions). Our results are in agreement with a recent study which showed that gD and the capsid protein VP5 colocalize with the 275-kDa mannose-6-phosphate receptor and the transferrin receptor (12). However, the significance of that finding for productive virus assembly was not addressed.

Since we failed to detect HSV particles in the Golgi apparatus, they may have reached TGN and/or endosomal compartments by a route other than the classical secretory pathway. The simplest interpretation of our data is that enveloped capsids accumulate within these organelles by budding into them from the cytoplasm. Consistent with this notion, biochemical analysis and electron microscopic inspection revealed that peak I organelles contained both lumenal enveloped virions and peripherally attached capsids, resembling structures previously observed by thin-section analysis of herpesvirus-infected cells (29, 39, 71, 72, 78, 84). That the nonenveloped peripherally attached capsids are on a productive pathway is consistent with their abundance (biochemical assays indicated that membrane-attached capsids were similar in abundance to enveloped ones) and the kinetics of their accumulation (during a synchronized wave of assembly they could be detected as early as infectious virions). It is also worth noting that these capsids were biochemically defined by their ability to protect the viral genome from DNase I digestion. They are therefore unlikely to be damaged or degraded, as pointed out for some populations of cytoplasmic capsid (72). Envelopment of HSV at the TGN was predicted by Griffiths and Rottier (32), but cytomegalovirus has been reported to envelope at endosomal membranes (71).

Envelopment at TGN and/or endosomes is consistent with the finding that ER-retained gH and gD are not incorporated into the viral envelope (11, 79) and also with envelope incorporation of TGN-targeted gD (79), which cycles between TGN and plasma membrane in endosomes (9, 37). This model for envelopment predicts that all of the membrane proteins found in the mature HSV particle must traffic through TGN/endosomes too, but there is only limited information concerning recycling of HSV envelope proteins (1, 12). For pseudorabies virus, it is clear that removal of the endocytosis motif from gE does not prevent its incorporation into viral particles (69, 70).

Direct envelopment of capsids at the TGN or endosomes is at odds with data showing enveloped virions in transit through the Golgi (72), but this study did not report what proportion of the total viral population was Golgi associated. TGN/endosomal envelopment would also appear to contradict the finding that gD, when retained in the *trans*-Golgi using the membrane span of sialyltransferase, still became assembled into the HSV envelope (53, 79). These data can, however, be reconciled in a number of ways. First, the distribution of the gD-sialyltransferase fusion protein within the Golgi stack was not tested by Whiteley and colleagues (79). It is possible that, in the context of an HSV-infected cell, not all of the fusion protein is tightly localized to the *trans* cisternae; some may have reached later compartments of the Golgi or endosomes. Furthermore, sialyltransferase has been reported to be an enzyme of both the *trans*-Golgi and TGN in some cell types (19, 64).

An alternative interpretation of our data is to suppose that enveloped HSV does pass through the ER and Golgi en route to TGN/endosomes but traverses these organelles so rapidly under our conditions that it never accumulates within them. We are currently testing this hypothesis by examining synchronized egress at lower temperatures to reduce the rate of trafficking. In this case, membrane-bound cytoplasmic capsids could well be the products of erroneous fusion between the HSV envelope and the bounding membrane (14, 27). Alternatively, it may be important to consider that our synchronized assembly studies were conducted at relatively early times postinfection: perhaps HSV preferentially accumulates within TGN/endosomes at early times, but at later time points occupies other organelles such as the earlier cisternae of the Golgi. Furthermore, HSV may utilize Golgi and TGN/endosomes to various extents in different cell lines; some of the effects of HSV infection on cytoplasmic organelles are clearly cell type dependent (3, 13).

In summary, we believe our data are most consistent with the notion that TGN or endosomes are the principal destination for trafficking HSV during a single wave of egress and that an acidic pH is important for the acquisition or maintenance of infectivity in these compartments. It remains unclear whether this requirement reflects some acid-dependent processing event critical for maturation or the absence from the organelle of essential proteins or lipids. Experiments are currently under way to distinguish between these possibilities and to determine the reason for the defect in particle infectivity.

ACKNOWLEDGMENTS

This work was supported by National Institutes of Health grants AI38265 and DK41918 to D.W.W. Core support was provided by NIH Cancer Center grant P30-CA13330.

We thank Lily Huang for technical assistance, Alex Morozov for help in the early stages of this work, and Allan Wolkoff, Richard Stockert, and numerous other members of the Einstein community for helpful discussions. We also gratefully acknowledge the Analytical Imaging Facility of the Albert Einstein College of Medicine for help with electron microscopy. The H4A3 hybridoma was developed by J.

August and J. Hildreth and obtained from the Developmental Studies Hybridoma Bank, established under the auspices of the NICHD at the University of Iowa. Antibodies against rab7 and p115 were kind gifts from Marino Zerial and Gerry Waters.

REFERENCES

1. **Alconada, A., U. Bauer, B. Sodeik, and B. Hoflack.** 1999. Intracellular traffic of herpes simplex virus glycoprotein gE: characterization of the sorting signals required for its *trans*-Golgi network localization. J. Virol. **73:**377–387.
2. **Andoh, T., H. Kawamata, M. Umatake, K. Terasawa, T. Takegami, and H. Ochiai.** 1998. Effect of bafilomycin A1 on the growth of Japanese encephalitis virus in Vero cells. J. Neurovirol. **4:**627–631.
3. **Avitabile, E., P. L. Ward, C. Di Lazzaro, M. R. Torrisi, B. Roizman, and G. Campadelli-Fiume.** 1994. The herpes simplex virus UL20 protein compensates for the differential disruption of exocytosis of virions and viral membrane glycoproteins associated with fragmentation of the Golgi apparatus. J. Virol. **68:**7397–7405.
4. **Banfield, B. W., and F. Tufaro.** 1990. Herpes simplex virus particles are unable to traverse the secretory pathway in the mouse L-cell mutant gro29. J. Virol. **64:**5716– 5729.
5. **Banfield, W. J., and A. L. Kisch.** 1973. The effect of chloroquine on herpesvirus infection in vitro and in vivo. Proc. Soc. Exp. Biol. Med. **142:**1018–1022.
6. **Bayer, N., D. Schober, E. Prchla, R. F. Murphy, D. Blaas, and R. Fuchs.** 1998. Effect of bafilomycin A1 and nocodazole on endocytic transport in HeLa cells: implications for viral uncoating and infection. J. Virol. **72:**9645–9655.
7. **Beckers, C. J., D. S. Keller, and W. E. Balch.** 1987. Semi-intact cells permeable to macromolecules: use in reconstitution of protein transport from the endoplasmic reticulum to the Golgi complex. Cell **50:**523–534.
8. **Benzi, L., P. Cecchetti, A. M. Ciccarone, A. Nardone, E. Merola, R. Maggiorelli, F. Campi, G. Di Cianni, and R. Navalesi.** 1997. Inhibition of endosomal acidification in normal cells mimics the derangements of cellular insulin and insulin-receptor metabolism observed in non-insulin-dependent diabetes mellitus. Metab. Clin. Exp. **46:**1259–1265.
9. **Bos, K., C. Wraight, and K. K. Stanley.** 1993. TGN38 is maintained in the trans-Golgi network by a tyrosine-containing motif in the cytoplasmic domain. EMBO J. **12:**2219–2228.
10. **Bowman, E. J., A. Siebers, and K. Altendorf.** 1988. Bafilomycins: a class of inhibitors of membrane ATPases from microorganisms, animal cells, and plant cells. Proc. Natl. Acad. Sci. USA **85:**7972–7976.
11. **Browne, H., S. Bell, T. Minson, and D. W. Wilson.** 1996. An endoplasmic reticulum-retained herpes simplex virus glycoprotein H is absent from secreted virions: evidence for reenvelopment during egress. J. Virol. **70:**4311–4316.
12. **Brunetti, C. R., K. S. Dingwell, C. Wale, F. L. Graham, and D. C. Johnson.** 1998. Herpes simplex virus gD and virions accumulate in endosomes by mannose 6-phosphate-dependent and -independent mechanisms. J. Virol. **72:**3330–3339.
13. **Campadelli, G., R. Brandimarti, C. Di Lazzaro, P. L. Ward, B. Roizman, and M. R. Torrisi.** 1993. Fragmentation and dispersal of Golgi proteins and redistribution of glycoproteins and glycolipids processed through the Golgi apparatus after infection with herpes simplex virus 1. Proc. Natl. Acad. Sci. USA **90:**2798–2802.
14. **Campadelli-Fiume, G., F. Farabegoli, S. Di Gaeta, and B. Roizman.** 1991. Origin of unenveloped capsids in the cytoplasm of cells infected with herpes simplex virus 1. J. Virol. **65:**1589–1595.
15. **Card, J. P., L. Rinaman, R. B. Lynn, B. H. Lee, R. P. Meade, R. R. Miselis, and L. W. Enquist.** 1993. Pseudorabies virus infection of the rat central nervous system: ultrastructural characterization of viral replication, transport, and pathogenesis. J. Neurosci. **13:**2515–2539.
16. **Chaney, W., S. Sundaram, N. Friedman, and P. Stanley.** 1989. The Lec4A CHO glycosylation mutant arises from miscompartmentalization of a Golgi glycosyltransferase. J. Cell Biol. **109:**2089–2096.
17. **Chapman, R. E., and S. Munro.** 1994. Retrieval of TGN proteins from the cell surface requires endosomal acidification. EMBO J. **13:**2305–2312.
18. **Chavrier, P., and B. Goud.** 1999. The role of ARF and Rab GTPases in membrane transport. Curr. Opin. Cell Biol. **11:**466–475.
19. **Chen, C., J. Ma, A. Lazic, M. Backovic, and K. J. Colley.** 2000. Formation of insoluble oligomers correlates with ST6GalI stable localization in the Golgi. J. Biol. Chem. **275:**13819–13826.
20. **Cheung, P., B. W. Banfield, and F. Tufaro.** 1991. Brefeldin A arrests the maturation and egress of herpes simplex virus particles during infection. J. Virol. **65:**1893–1904.
21. **Chi, J. H., and D. W. Wilson.** 2000. ATP-dependent localization of the herpes simplex virus capsid protein VP26 to sites of procapsid maturation. J. Virol. **74:**1468–1476.
22. **Church, G. A., A. Dasgupta, and D. W. Wilson.** 1998. Herpes simplex virus DNA packaging without measurable DNA synthesis. J. Virol. **72:**2745–2751.
23. **Church, G. A., and D. W. Wilson.** 1997. Study of herpes simplex virus maturation during a synchronous wave of assembly. J. Virol. **71:**3603–3612.
24. **Dasgupta, A., and D. W. Wilson.** 1999. ATP depletion blocks herpes simplex virus DNA packaging and capsid maturation. J. Virol. **73:**2006–2015.
25. **Di Lazzaro, C., G. Campadelli-Fiume, and M. R. Torrisi.** 1995. Intermediate forms of glycoconjugates are present in the envelope of herpes simplex virions during their transport along the exocytic pathway. Virology **214:**619–623.
26. **Dinter, A., and E. G. Berger.** 1998. Golgi-disturbing agents. Histochem. Cell Biol. **109:**571–590.
27. **Enquist, L. W., P. J. Husak, B. W. Banfield, and G. A. Smith.** 1998. Infection and spread of alphaherpesviruses in the nervous system. Adv. Virus Res. **51:**237–347.
28. **Gao, M., L. Matusick-Kumar, W. Hurlburt, S. F. DiTusa, W. W. Newcomb, J. C. Brown, P. J. McCann, 3rd, I. Deckman, and R. J. Colonno.** 1994. The protease of herpes simplex virus type 1 is essential for functional capsid formation and viral growth. J. Virol. **68:**3702–3712.
29. **Gershon, A. A., D. L. Sherman, Z. Zhu, C. A. Gabel, R. T. Ambron, and M. D. Gershon.** 1994. Intracellular transport of newly synthesized varicella-zoster virus: final envelopment in the *trans*-Golgi network. J. Virol. **68:**6372–6390.
30. **Granzow, H., F. Weiland, A. Jons, B. G. Klupp, A. Karger, and T. C. Mettenleiter.** 1997. Ultrastructural analysis of the replication cycle of pseudorabies virus in cell culture: a reassessment. J. Virol. **71:**2072–2082.
31. **Griffiths, G., R. Pepperkok, J. K. Locker, and T. E. Kreis.** 1995. Immunocytochemical localization of β-COP to the ER-Golgi boundary and the TGN. J. Cell Sci. **108:**2839–2856.
32. **Griffiths, G., and P. Rottier.** 1992. Cell biology of viruses that assemble along the biosynthetic pathway. Semin. Cell Biol. **3:**367–381.
33. **Harford, J., K. Bridges, G. Ashwell, and R. D. Klausner.** 1983. Intracellular dissociation of receptor-bound asialoglycoproteins in cultured hepatocytes: a pH-mediated nonlysosomal event. J. Biol. Chem. **258:**3191–3197.
34. **Harson, R., and C. Grose.** 1995. Egress of varicella-zoster virus from the melanoma cell: a tropism for the melanocyte. J. Virol. **69:**4994–5010.
35. **Holland, D. J., A. L. Cunningham, and R. A. Boadle.** 1998. The axonal transmission of herpes simplex virus to epidermal cells: a novel use of the freeze substitution technique applied to explant cultures retained on cover slips. J. Microsc. **192:**69–72.
36. **Holland, D. J., M. Miranda-Saksena, R. A. Boadle, P. Armati, and A. L. Cunningham.** 1999. Anterograde transport of herpes simplex virus proteins in axons of peripheral human fetal neurons: an immunoelectron microscopy study. J. Virol. **73:**8503–8511.
37. **Humphrey, J. S., P. J. Peters, L. C. Yuan, and J. S. Bonifacino.** 1993. Localization of TGN38 to the *trans*-Golgi network: involvement of a cytoplasmic tyrosine-containing sequence. J. Cell Biol. **120:**1123–1135.
38. **Johnson, D. C., and P. G. Spear.** 1982. Monensin inhibits the processing of herpes simplex virus glycoproteins, their transport to the cell surface, and the egress of virions from infected cells. J. Virol. **43:**1102–1112.
39. **Jones, F., and C. Grose.** 1988. Role of cytoplasmic vacuoles in varicella-zoster virus glycoprotein trafficking and virion envelopment. J. Virol. **62:**2701–2711.
40. **Kelman, Z.** 1997. PCNA: structure, functions and interactions. Oncogene **14:**629–640.
41. **Komuro, M., M. Tajima, and K. Kato.** 1989. Transformation of Golgi membrane into the envelope of herpes simplex virus in rat anterior pituitary cells. Eur. J. Cell Biol. **50:**398–406.
42. **Kousoulas, K. G., D. J. Bzik, N. DeLuca, and S. Person.** 1983. The effect of ammonium chloride and tunicamycin on the glycoprotein content and infectivity of herpes simplex virus type 1. Virology **125:**468–474.
43. **Kousoulas, K. G., S. Person, and T. C. Holland.** 1982. Herpes simplex virus type 1 cell fusion occurs in the presence of ammonium chloride-inhibited glycoproteins. Virology **123:**257–263.
44. **Koyama, A. H., and A. Adachi.** 1997. Induction of apoptosis by herpes simplex virus type 1. J. Gen. Virol. **78:**2909–2912.
45. **Koyama, A. H., and T. Uchida.** 1984. Inhibition of multiplication of herpes simplex virus type 1 by ammonium chloride and chloroquine. Virology **138:**332–335.
46. **Lancz, G. J., L. C. McLaren, C. G. James, and J. V. Scaletti.** 1971. Chloroquine mediated alterations in mammalian cell metabolism and viral replication. Proc. Soc. Exp. Biol. Med. **136:**1289–1293.
47. **Lippincott-Schwartz, J., L. Yuan, C. Tipper, M. Amherdt, L. Orci, and R. Klausner.** 1991. Brefeldin A's effects on endosomes, lysosomes, and the TGN suggest a general mechanism for regulating organelle structure and membrane traffic. Cell **67:**601–616.
48. **Liu, F. Y., and B. Roizman.** 1991. The herpes simplex virus 1 gene encoding a protease also contains within its coding domain the gene encoding the more abundant substrate. J. Virol. **65:**5149–5156.
49. **Miranda-Saksena, M., P. Armati, R. A. Boadle, D. J. Holland, and A. L. Cunningham.** 2000. Anterograde transport of herpes simplex virus type 1 in cultured, dissociated human and rat dorsal root ganglion neurons. J. Virol. **74:**1827–1839.
50. **Mohrmann, K., and P. van der Sluijs.** 1999. Regulation of membrane transport through the endocytic pathway by rab GTPases. Mol. Membr. Biol. **16:**81–87.
51. **Montalvo, E. A., R. T. Parmley, and C. Grose.** 1986. Varicella-zoster viral

glycoprotein envelopment: ultrastructural cytochemical localization. J. Histochem. Cytochem. **34:**281–284.
52. **Mu, F. T., J. M. Callaghan, O. Steele-Mortimer, H. Stenmark, R. G. Parton, P. L. Campbell, J. McCluskey, J. P. Yeo, E. P. Tock, and B. H. Toh.** 1995. EEA1, an early endosome-associated protein: EEA1 is a conserved alpha-helical peripheral membrane protein flanked by cysteine "fingers" and contains a calmodulin-binding IQ motif. J. Biol. Chem. **270:**13503–13511.
53. **Munro, S.** 1991. Sequences within and adjacent to the transmembrane segment of alpha-2, 6-sialyltransferase specify Golgi retention. EMBO J. **10:**3577–3588.
54. **Newcomb, W. W., B. L. Trus, N. Cheng, A. C. Steven, A. K. Sheaffer, D. J. Tenney, S. K. Weller, and J. C. Brown.** 2000. Isolation of herpes simplex virus procapsids from cells infected with a protease-deficient mutant virus. J. Virol. **74:**1663–1673.
55. **Penfold, M. E., P. Armati, and A. L. Cunningham.** 1994. Axonal transport of herpes simplex virions to epidermal cells: evidence for a specialized mode of virus transport and assembly. Proc. Natl. Acad. Sci. USA **91:**6529–6533.
56. **Prescott, A. R., J. M. Lucocq, J. James, J. M. Lister, and S. Ponnambalam.** 1997. Distinct compartmentalization of TGN46 and beta 1,4-galactosyltransferase in HeLa cells. Eur. J. Cell Biol. **72:**238–246.
57. **Preston, V. G., J. A. Coates, and F. J. Rixon.** 1983. Identification and characterization of a herpes simplex virus gene product required for encapsidation of virus DNA. J. Virol. **45:**1056–1064.
58. **Rixon, F. J., A. M. Cross, C. Addison, and V. G. Preston.** 1988. The products of herpes simplex virus type 1 gene UL26 which are involved in DNA packaging are strongly associated with empty but not with full capsids. J. Gen. Virol. **69:**2879–2891.
59. **Rixon, F. J., and D. McNab.** 1999. Packaging-competent capsids of a herpes simplex virus temperature-sensitive mutant have properties similar to those of in vitro-assembled procapsids. J. Virol. **73:**5714–5721.
60. **Robinson, M. S.** 1990. Cloning and expression of gamma-adaptin, a component of clathrin-coated vesicles associated with the Golgi apparatus. J. Cell Biol. **111:**2319–2326.
61. **Rohrer, J., A. Schweizer, D. Russell, and S. Kornfeld.** 1996. The targeting of Lampl to lysosomes is dependent on the spacing of its cytoplasmic tail tyrosine sorting motif relative to the membrane. J. Cell Biol. **132:**565–576.
62. **Roizman, B. and A. E. Sears.** 1993. Herpes simplex viruses and their replication, p. 11–68. *In* B. Roizman, R. J. Whitley, and C. Lopez (ed.), The human herpesviruses. Raven Press, Ltd., New York, N.Y.
63. **Roizman, B., and A. E. Sears.** 1996. Herpes simplex viruses and their replication, p. 2231–2295. *In* B. N. Fields, D. M. Knipe, and P. M. Howley (ed.), Fields virology, 3rd ed. Lippincott-Raven Publishers, Philadelphia, Pa.
64. **Roth, J., D. J. Taatjes, J. M. Lucocq, J. Weinstein, and J. C. Paulson.** 1985. Demonstration of an extensive trans-tubular network continuous with the Golgi apparatus stack that may function in glycosylation. Cell **43:**287–295.
65. **Stackpole, C. W.** 1969. Herpes-type virus of the frog renal adenocarcinoma. I. Virus development in tumor transplants maintained at low temperature. J. Virol. **4:**75–93.
66. **Stephens, E. B., and R. W. Compans.** 1988. Assembly of animal viruses at cellular membranes. Annu. Rev. Microbiol. **42:**489–516.
67. **Strous, G., P. van Kerkhof, G. van Meer, S. Rijnboutt, and W. Stoorvogel.** 1993. Differential effects of brefeldin A on transport of secretory and lysosomal proteins. J. Biol. Chem. **268:**2341–2347.
68. **Strous, G. J., E. G. Berger, P. van Kerkhof, H. Bosshart, B. Berger, and H. J. Geuze.** 1991. Brefeldin A induces a microtubule-dependent fusion of galactosyltransferase-containing vesicles with the rough endoplasmic reticulum. Biol. Cell **71:**25–31.
69. **Tirabassi, R. S., and L. W. Enquist.** 1999. Mutation of the YXXL endocytosis motif in the cytoplasmic tail of pseudorabies virus gE. J. Virol. **73:**2717–2728.
70. **Tirabassi, R. S., and L. W. Enquist.** 1998. Role of envelope protein gE endocytosis in the pseudorabies virus life cycle. J. Virol. **72:**4571–4579.
71. **Tooze, J., M. Hollinshead, B. Reis, K. Radsak, and H. Kern.** 1993. Progeny vaccinia and human cytomegalovirus particles utilize early endosomal cisternae for their envelopes. Eur. J. Cell Biol. **60:**163–178.
72. **Torrisi, M. R., C. Di Lazzaro, A. Pavan, L. Pereira, and G. Campadelli-Fiume.** 1992. Herpes simplex virus envelopment and maturation studied by fracture label. J. Virol. **66:**554–561.
73. **Trombetta, E. S., and A. Helenius.** 1998. Lectins as chaperones in glycoprotein folding. Curr. Opin. Struct. Biol. **8:**587–592.
74. **Vahlne, A. G., and J. Blomberg.** 1974. Purification of herpes simplex virus. J. Gen. Virol. **22:**297–302.
75. **Vahro, M., and W. Slenczka.** 1979. Rapid purification of lymphocytic choriomeningitis virus by density gradient centrifugation in colloidal silica. J. Gen. Virol. **42:**215–218.
76. **van Genderen, I. L., R. Brandimarti, M. R. Torrisi, G. Campadelli, and G. van Meer.** 1994. The phospholipid composition of extracellular herpes simplex virions differs from that of host cell nuclei. Virology **200:**831–836.
77. **Waters, M. G., D. O. Clary, and J. E. Rothman.** 1992. A novel 115-kD peripheral membrane protein is required for intercisternal transport in the Golgi stack. J. Cell Biol. **118:**1015–1026.
78. **Whealy, M. E., J. P. Card, R. P. Meade, A. K. Robbins, and L. W. Enquist.** 1991. Effect of brefeldin A on alphaherpesvirus membrane protein glycosylation and virus egress. J. Virol. **65:**1066–1081.
79. **Whiteley, A., B. Bruun, T. Minson, and H. Browne.** 1999. Effects of targeting herpes simplex virus type 1 gD to the endoplasmic reticulum and *trans*-Golgi network. J. Virol. **73:**9515–9520.
80. **Whittaker, G. R., and A. Helenius.** 1998. Nuclear import and export of viruses and virus genomes. Virology **246:**1–23.
81. **Wood, S. A., J. E. Park, and W. J. Brown.** 1991. Brefeldin A causes a microtubule-mediated fusion of the trans-Golgi network and early endosomes. Cell **67:**591–600.
82. **Yamamoto, A., Y. Tagawa, T. Yoshimori, Y. Moriyama, R. Masaki, and Y. Tashiro.** 1998. Bafilomycin A1 prevents maturation of autophagic vacuoles by inhibiting fusion between autophagosomes and lysosomes in rat hepatoma cell line, H-4-II-E cells. Cell Struct. Funct. **23:**33–42.
83. **Yoshimori, T., A. Yamamoto, Y. Moriyama, M. Futai, and Y. Tashiro.** 1991. Bafilomycin A1, a specific inhibitor of vacuolar-type H^+-ATPase, inhibits acidification and protein degradation in lysosomes of cultured cells. J. Biol. Chem. **266:**17707–17712.
84. **Zhu, Z., M. D. Gershon, Y. Hao, R. T. Ambron, C. A. Gabel, and A. A. Gershon.** 1995. Envelopment of varicella-zoster virus: targeting of viral glycoproteins to the *trans*-Golgi network. J. Virol. **69:**7951–7959.